An intramolecular charge transfer state of carbonyl carotenoids: Implications for excited state dynamics of apo-carotenals and retinal

4 AUTHORS, INCLUDING:

Tomás Polívka
University of South Bohemia in České Bud…
113 PUBLICATIONS **4,151** CITATIONS

SEE PROFILE

Pavel Chabera
Lund University
39 PUBLICATIONS **771** CITATIONS

SEE PROFILE

An intramolecular charge transfer state of carbonyl carotenoids: implications for excited state dynamics of apo-carotenals and retinal

Tomáš Polívka,[*ab] **Shanti Kaligotla,**[c] **Pavel Chábera†[a] and Harry A. Frank[c]**

Excited state dynamics of two apo-carotenals, retinal and 12′-apo-β-carotenal, were studied by femtosecond transient absorption spectroscopy. We make use of previous knowledge gathered from studies of various carbonyl carotenoids and suggest that to consistently explain the excited-state dynamics of retinal in polar solvents, it is necessary to include an intermolecular charge transfer (ICT) state in the excited state manifold. Coupling of the ICT state to the A_g^- state, which occurs in polar solvents, shortens lifetime of the lowest excited state of 12′-apo-β-carotenal from 180 ps in *n*-hexane to 7.1 ps in methanol. Comparison with a reference molecule lacking the conjugated carbonyl group, 12′-apo-β-carotene, demonstrates the importance of the carbonyl group; no polarity-induced lifetime change is observed and 12′-apo-β-carotene decays to the ground state in 220 ps regardless of solvent polarity. For retinal, we have confirmed the well-known three-state relaxation scheme in *n*-hexane. Population of the B_u^+ state decays in <100 fs to the A_g^- state, which is quenched in 440 fs by a low-lying nπ* state that decays with a 33 ps time constant to form the retinal triplet state. In methanol, however, the A_g^- state is coupled to the ICT state. This coupling prevents population of the nπ* state, which explains the absence of retinal triplet formation in polar solvents. Instead, the coupled A_g^-/ICT state decays in 1.6 ps to the ground state. The A_g^-/ICT coupling is also evidenced by stimulated emission, which is a characteristic marker of the ICT state in carbonyl carotenoids.

Introduction

Carotenoids are a class of natural pigments that exhibit complex photophysics involving both allowed and forbidden excited states.[1] The molecules formally belong to the C_{2h} point group that contains the irreducible symmetry representations, B_u and A_g.[2] It has been known for nearly 40 years[3] that the lowest excited state S_1 has the same symmetry (A_g^-) as the ground state, S_0, which renders the S_0–S_1 transition forbidden for one-photon transitions. The characteristic strong absorption band of carotenoids in the blue-green spectral region is due to a transition from the ground state to an excited state having B_u^+ symmetry. Historically, this has been denoted the S_2 state. Thus, when a carotenoid molecule is excited into the S_2 state, it undergoes internal conversion to populate the S_1 state within a few hundred femtoseconds, and the S_1 state subsequently decays on a picosecond time scale to the ground state.[1]

This three-state model involving S_0 (A_g^-), S_1 (A_g^-) and S_2 (B_u^+) served as the standard for a description of carotenoid photophysics until about ten years ago when various experimental and theoretical findings suggested that additional dark excited states may be involved in controlling the deactivation of the excited states of the molecules.[1,4]

An intramolecular charge transfer (ICT) state is among the dark states of carotenoids that may be playing a role in excited state deactivation. Its presence requires that a carbonyl group be conjugated with the π-electron system of double bonds.[5,6] The ICT state was first reported for the highly substituted carbonyl carotenoid peridinin,[7] and subsequently identified as a common feature in many other carbonyl carotenoids.[5–9] The presence of the ICT state is characterized by a significant dependence of the excited state spectra and dynamics on the polarity of the environment. In polar solvents, the ICT state is stabilized, and new spectral bands appear in the transient absorption spectrum. In addition, the lifetime of the lowest excited state becomes markedly shorter compared to its value in nonpolar solvents. A close interaction between the S_1 and ICT states gives rise to these effects, and this has led to the notation S_1/ICT for the combined system of states.[10,11]

Ultrafast time-resolved spectroscopic experiments have established that these effects are stronger in carbonyl carotenoids having short π-electron conjugation lengths: whereas carbonyl

[a] Institute of Physical Biology, University of South Bohemia, Zámek 136, 373 33 NovéHrady, Czech Republic. E-mail: polivka@ufb.jcu.cz
[b] Institute of Plant Molecular Biology, Biological Centre, Czech Academy of Sciences, Czech Republic
[c] Department of Chemistry, 55 North Eagleville Road, University of Connecticut, Storrs, CT 06269-3060, USA
† Current address: Department of Chemical Physics, Lund University, Sweden.

carotenoids having a conjugated chain consisting of 10 or more carbon–carbon double bonds usually do not exhibit any dependence of the S_1/ICT lifetime on solvent polarity,[5,12,13] for shorter carotenoids the S_1/ICT lifetime in nonpolar and polar solvents can differ by more than an order of magnitude.[14–16] It has also been established that in order to observe an ICT state-induced effect on the excited state dynamics of carotenoids, the conjugated carbonyl group must be positioned asymmetrically with respect to the main conjugated backbone,[17] although in extremely high polarity solvents, carotenoids having two symmetric carbonyl groups can display a small ICT state-induced effect.[18] Recent quantum chemical calculations have suggested that the ICT state should be viewed as a dynamic feature generated within a few tens of femtoseconds after photo-excitation of the molecules, and that its formation requires extensive mixing of states having A_g^- and B_u^+ symmetry.[17]

Polarity-dependent excited-state dynamics have also been reported for a series of apo-carotenals which are synthetic carbonyl carotenoids having a single conjugated carbonyl group attached to the end of the C=C conjugated chain.[12,15,19–21] These molecules are ideal for probing the relationship between π-electron conjugation length, N, and polarity-induced effects, because their conjugation can be systematically varied. Three such apo-carotenals have been studied in detail so far: 12′-apo-β-carotenal whose conjugation length is here denoted as $N = 6\beta 1O$ due to its having 6 linear conjugated C=C bonds, one C=C bond in an s-cis orientation in a terminal β-ring, and one conjugated C=O bond attached to the end of the conjugated chain (Fig. 1); 8′-apo-β-carotenal ($N = 8\beta 1O$); and 4′-apo-β-carotenal ($N = 10\beta 1O$). The experiments showed that in nonpolar solvents the transient absorption spectra exhibit a single dominant band characteristic of the S_1–S_n excited state transition of carotenoids.[21] Moreover, the S_1 lifetime followed the energy gap law for radiationless transitions[22] previously applied to carotenoids;[23,24] the longer the carotenoid, the smaller the S_0–S_1 energy gap, and consequently, the shorter the S_1 lifetime. In the nonpolar solvent, n-hexane, the S_1 lifetimes were reported to be 4.7 ps (4′-apo-β-carotenal), 21 ps (8′-apo-β-carotenal) and 190 ps (12′-apo-β-carotenal).[12,15,19,21]
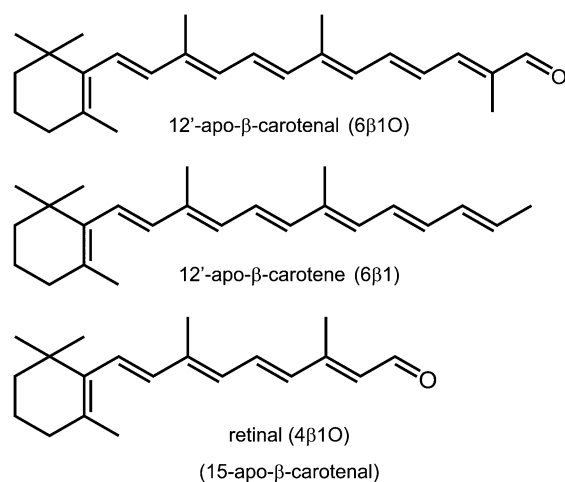

Fig. 1 Molecular structures of 12′-apo-β-carotenal, 12′-apo-β-carotene and retinal.

In the polar solvent, methanol, however, due to coupling of the S_1 and ICT states, the S_1/ICT lifetime became significantly shorter in 8′-apo-β-carotenal and 12′-apo-β-carotenal, yielding ~8 ps in both molecules.[12,15,20,21] No lifetime shortening was observed for the longest carotenoid in the series, 4′-apo-β-carotenal.[12] A mild effect was observed for 6′-apo-β-carotenal ($N = 9\beta 1O$) for which it was reported that its 12 ps lifetime in n-hexane was shortened to 6.5 ps in methanol.[25] In addition, new spectral bands associated with the ICT state appeared in the transient absorption spectrum of 12′-apo-β-carotenal.[21] Thus, it can be concluded that the influence of the ICT state on the excited-state dynamics increases with decreasing π-electron conjugation length of apo-carotenals.

It is interesting to note that the next shorter molecule in the series of apo-carotenals described above is 15-apo-β-carotenal, better known as retinal ($N = 4\beta 1O$, Fig. 1). Retinal is of profound interest because it is the chromophore that triggers the photocycle in rhodopsin-type photoreceptors.[26] Retinal has a similar excited state complexion as longer chain carotenoids, and contains both allowed B_u^+ and forbidden A_g^- states, but due to its very short conjugation, an nπ* state derived from the presence of the carbonyl group falls below the strongly-absorbing B_u^+ state.[27] This aspect further complicates the excited state dynamics of the molecule. It is now accepted that for retinal dissolved in nonpolar solvents such as n-hexane, the lowest excited state (denoted S_1) is the nπ* state.[28,29] This dramatically changes the excited-state dynamics compared with longer apo-carotenals which do not have a low-lying nπ* state; the excited B_u^+ state (for retinal usually denoted as S_3) decays in 56 fs[29] to the A_g^- state (S_2) whose lifetime is only 400 fs determined by internal conversion to the nπ* state.[28,29] The nπ* state then decays within 33 ps to a triplet state, which is readily identified by the characteristic T_1–T_n transition around 440 nm.[30]

In polar solvents, however, the excited state relaxation scheme following photoexcitation of retinal is less clear. Formation of the triplet state is significantly inhibited in 1-butanol,[30] ethanol,[31] and acetonitrile.[32] The kinetics recorded for retinal in polar solvents appeared to consist of two decay components of 200–300 fs and 1.6–1.8 ps that were assigned to lifetimes of the B_u^+ and A_g^- states, respectively.[30] Alternatively, Larson et al.[32] in a comparison of one- and two-photon excitation experiments proposed a more complex, 'reverse' kinetic scheme for retinal in polar solvents in which the B_u^+ state decays in 1.6–1.8 ps to the A_g^- state that then populates the nπ* state in 200–300 fs.[32] Although these relaxation schemes may explain the observed dynamics, it is hard to reconcile the B_u^+ lifetime in polar solvents being significantly longer (200–300 fs in ref. 30, 1.6–1.8 ps in ref. 32) than in nonpolar solvent. The energy gap between the B_u^+ and A_g^- states is only ~2400 cm^{-1},[33] and based on knowledge gathered from carbonyl carotenoids, this gap is only marginally affected by solvent polarity.[6,10] Moreover, none of the relaxation schemes proposed to explain the excited-state dynamics of retinal in polar solvents justifies the near absence of intersystem crossing to the triplet state.

Here we propose an alternate way of accounting for the excited-state dynamics of retinal in polar solvents. Following up on the reports on the behavior of a systematic series

of carbonyl-containing carotenoids[8,13,16,17] we compare the transient absorption spectra and dynamics recorded in polar and nonpolar solvents for retinal and its longer counterpart 12′-apo-β-carotenal. We show that the information gathered previously for the excited state dynamics of carbonyl carotenoids and especially apo-carotenals allows us to identify similar transient absorption species in retinal. Wherein, we demonstrate that the time-resolved data reported previously for retinal can be explained consistently by including an ICT state in the relaxation scheme. To stress the importance of the conjugated carbonyl group, we analyzed 12′-apo-β-carotene as a non-carbonyl reference molecule ($N = 6\beta1$, Fig. 1). In order to avoid confusion with state numbering for retinal and carotenoids that differs widely in the literature, we will use symmetry labels to denote the excited singlet states. Therefore, the S_1/ICT state of carbonyl carotenoids will be denoted as A_g^-/ICT, and the notation $A_g^- - nB_u^+$ will be used for the strongly allowed S_1–S_n transition of carotenoids because the S_n state is a higher-lying state of B_u^+ symmetry.

Materials and methods

All-*trans*-retinal was purchased from Sigma and 12′-apo-β-carotenal from Carotenature. 12′-Apo-β-carotene was prepared from retinal by the Wittig reaction. Crotylphosphonium bromide and NaH were suspended in THF. After flushing with nitrogen, it was stirred at 55 °C until hydrogen release stopped. At 4 °C, all-*trans*-retinal in THF was added dropwise. After stirring for 4 h at 55 °C, the solvent was removed at reduced pressure, the residue extracted with isohexane, and the extract filtered through silica. Drying and evaporating the organic solvent gave 12′-apo-β-carotene in a 38% yield, which was analyzed and purified using a Waters 600S HPLC system with a Nova-Pak C18 column. The flow rate was set at 1 mL min^{-1} and the mobile phase was programmed to be isocratic methanol/ethyl acetate (68/32 v/v). The samples were dried and stored at −80 °C. Prior to experiments, samples were dissolved in spectroscopic grade methanol or *n*-hexane to yield an optical density of 0.3–0.5 at the absorption maximum in a 1 mm cuvette.

The femtosecond spectrometer used for transient absorption measurements is based on a laser system Integra-i (Quantronix). It consists of Er-fiber oscillator and Ti:Sapphire amplifier producing ∼130 fs pulses centered at 790 nm at a repetition rate of 1 kHz. The amplified pulses were divided into two paths. The first was frequency-doubled in a BBO nonlinear crystal to produce excitation pulses centered at 395 nm. To obtain broadband white-light pulses for probing, a fraction of amplifier output was focused into continuously moving 2 mm CaF$_2$ plate. The resulting white-light continuum, which covers the spectral region from 400–700 nm, was collimated by an off-axis parabolic mirror and divided into the probe beam, which overlapped with the pump beam at the sample, and a reference beam that passes the sample outside the excited area. Probe and reference beams were focused to the sample by a pair of 30 cm spherical mirrors. After passing the sample, both beams were dispersed in spectrograph onto a double photodiode array with 1024 elements allowing measurements of transient spectra in a spectral window of ∼240 nm.

During all measurements, the excitation intensity was kept below 10^{15} photons pulse^{-1}·cm^{-2} to achieve a reasonable signal-to-noise ratio and to prevent sample degradation. The instrument response function was ∼130 fs as determined by fitting the instantaneous rise of a bleaching signal from a laser dye. The relative polarization of the pump and probe beams was set to the magic angle (54.7°) by placing a polarization rotator in the pump beam. All measurements were carried out in a rotating cuvette consisting of two 1 mm quartz windows separated by a 1 mm Teflon spacer.

Transient spectra collected by the diode-array detection system were fitted globally using DAFit software (Pascher Instruments) to a sum of exponentials, including numerical deconvolution of the response function, and a fourth degree polynomial describing the chirp. To visualize the excited state dynamics, we assume that the excited system evolves according to a sequential, irreversible scheme A → B, B → C, C → D... The arrows represent increasingly slower monoexponential processes and the time constants of these processes correspond to lifetimes of the species A, B, C, D... The spectral profiles of the species are called evolution-associated difference spectra (EADS), and provide information about the time evolution of the whole system.[34]

Results

Absorption spectra of the three molecules, retinal, 12′-apo-β-carotene and 12′-apo-β-carotenal, in the nonpolar solvent *n*-hexane and the polar solvent methanol are shown in Fig. 2. In both solvents, the absorption maximum, corresponding to the 0–1 vibrational transition of the absorption band, varies with the number of conjugated double bonds. The shortest molecule, retinal, having a conjugation length of 5 C=C bonds extended to a C=O group ($N = 4\beta1O$, Fig. 1), has an absorption maximum at 370 nm in *n*-hexane. The same value, 370 nm, is observed for 12′-apo-β-carotene, even though its conjugation length is supposedly longer ($N = 6\beta1$). However, a significant red-shift occurs for 12′-apo-β-carotenal whose absorption spectrum peaks at 415 nm in *n*-hexane. This observation is in agreement with previous studies showing that if the π-electron conjugation is extended to the carbonyl group, the energy of the absorbing B_u^+ state is always lower than for molecules with the same conjugation length consisting only of C=C bonds.[6] Thus, even if retinal has shorter conjugation than 12′-apo-β-carotene the presence of the conjugated carbonyl group in retinal pushes the B_u^+ state low enough to match the energy of the longer 12′-apo-β-carotene. The same effect causes the significant (∼3000 cm^{-1}) difference between the absorption maxima of 12′-apo-β-carotene and 12′-apo-β-carotenal, although they differ only by one C=O group.

An effect of polarity on the absorption spectra is also clearly related to the presence of the conjugated carbonyl group. Whereas the absorption spectra of 12′-apo-β-carotene taken in *n*-hexane and methanol are essentially identical, a polarity-induced red-shift indicating stabilization of the B_u^+ state in polar solvent is observed for retinal and 12′-apo-β-carotenal; their absorption spectra peaks at 380 and 428 nm, respectively. In addition, the characteristic polarity-induced effects, loss of
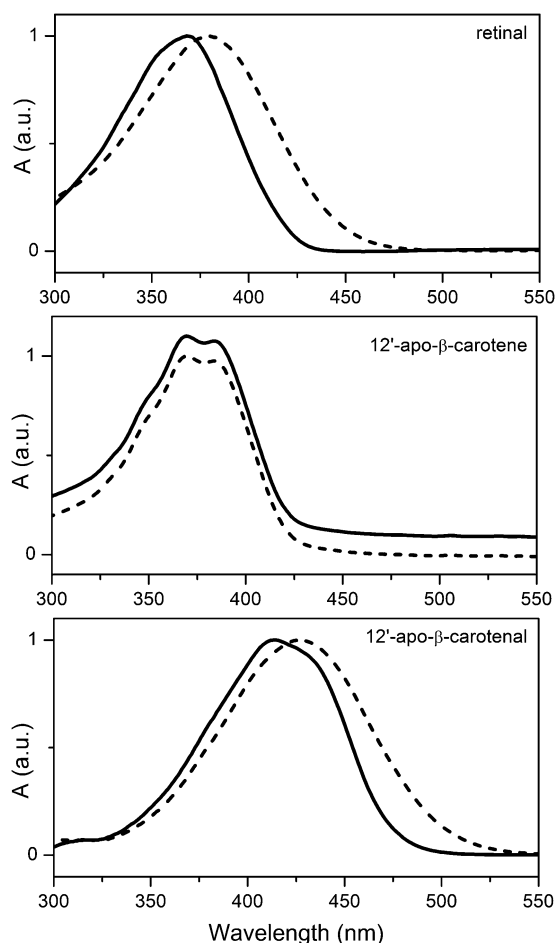
This journal is © the Owner Societies 2011

Phys. Chem. Chem. Phys., 2011, **13**, 10787–10796 | 10789

Fig. 2 Absorption spectra of the carotenoids in *n*-hexane (solid) and methanol (dashed). For 12′-apo-β-carotene the absorption spectrum in *n*-hexane was moved vertically to distinguish the spectra in the two solvents.

vibronic structure, and asymmetric broadening of the absorption band, are obvious in the absorption spectra of retinal and 12′-apo-β-carotenal (Fig. 2). These effects were observed earlier for a number of carbonyl carotenoids,[5,6] including 12′-apo-β-carotenal,[15,20] and they are considered to be typical indicators that ICT state is involved in excited-state dynamics. It is important to note that although the polarity-induced effects on the absorption spectrum of retinal are the same as those on 12′-apo-β-carotenal (Fig. 2), the ICT state has never been considered for explaining the excited-state dynamics of retinal in polar solvents.[30,32]

Further effects indicating the influence of the conjugated carbonyl group on the excited-state properties of retinal are demonstrated in the transient absorption data. All transient absorption data were recorded with excitation at 395 nm, which excites the low-energy tail of absorption spectra of retinal and 12′-apo-β-carotene. For 12′-apo-β-carotenal excitation at 395 nm provides excess energy as this excitation wavelength is approximately resonant with the 0–3 vibronic band of the B_u^+ state. Although this excess excitation energy usually affects the initial dynamics associated with the B_u^+ state,[35] and in the specific case of the carbonyl-containing carotenoid peridinin, it was shown that the lifetime of the ICT state is excitation

wavelength dependent,[11] earlier experiments with 12′-apo-β-carotenal measured in a few solvents including methanol demonstrated that excitation into higher vibrational levels of the B_u^+ state has negligible effect on the resulting excited-state dynamics.[19]

Transient absorption spectra of 12′-apo-β-carotene measured in both solvents are shown in Fig. 3. The transient spectra further underline similarity of spectroscopic properties in polar and non-polar solvents. Both transient absorption spectra are nearly identical, dominated by the characteristic $A_g^- - nB_u^+$ transition (the so-called S_1–S_n band) peaking at 465 nm (methanol) and 467 nm (*n*-hexane). Also, kinetics recorded at the maximum of the $A_g^- - nB_u^+$ transition (Fig. 3a, inset) in both solvents exhibit the same decay times. Global fitting of the whole dataset obtained for 12′-apo-β-carotene in methanol (Fig. 3b) provides three kinetic components that are associated with decay of the B_u^+ state (100 fs), relaxation of the hot A_g^- state (2.5 ps), and decay of the relaxed A_g^- state to the ground state (220 ps). The same components were obtained also from global fitting the data recorded for 12′-apo-β-carotene in *n*-hexane (not shown).

Transient absorption spectra of 12′-apo-β-carotenal in *n*-hexane (Fig. 4a) resemble those of 12′-apo-β-carotene except the $A_g^- - nB_u^+$ transition is red-shifted, peaking for 12′-apo-β-carotenal at 510 nm. Kinetics at the maximum of the $A_g^- - nB_u^+$ transition decays with a time constant of 180 ps (see global fitting described below), which is faster than for 12′-apo-β-carotene, and which most likely results from a slightly longer
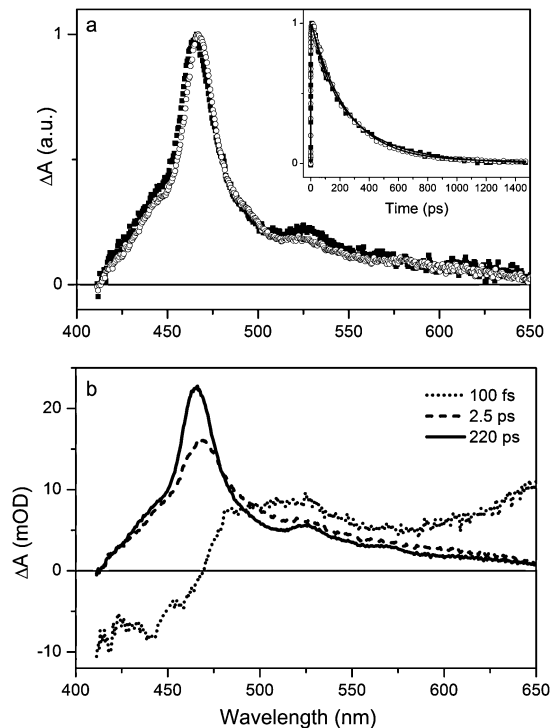

Fig. 3 (a) Transient absorption spectra of 12′-apo-β-carotene in methanol (full symbols) and *n*-hexane (open symbols). Both spectra are measured at 70 ps after excitation at 395 nm and normalized to maximum. Inset shows normalized kinetics in both solvents recorded at 465 nm. (b) EADS obtained from global fitting data recorded for 12′-apo-β-carotene in methanol.
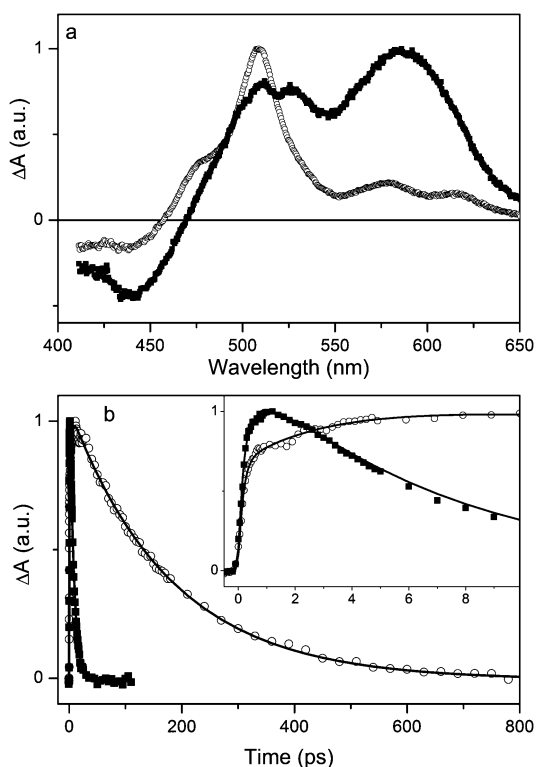
Fig. 4 (a) Transient absorption spectra of 12′-apo-β-carotenal in methanol (full symbols) and *n*-hexane (open symbols). Spectra are measured at 4 ps (*n*-hexane) and 1 ps (methanol). (b) Kinetics of 12′-apo-β-carotenal in methanol (full symbols, 590 nm) and *n*-hexane (open symbols, 510 nm). Inset shows dynamics within the first 10 ps.

Fig. 5 EADS obtained from global fitting the data measured for 12′-apo-β-carotenal in *n*-hexane (a) and methanol (b).

effective conjugation of 12′-apo-β-carotenal. Unlike 12′-apo-β-carotene, however, transient absorption spectra of 12′-apo-β-carotenal in *n*-hexane contain weak, but clearly pronounced, bands in the 550–650 nm region. These bands have been observed for a number of carbonyl carotenoids in nonpolar solvents[5,6,17,21] and are indicative of the ICT state being present in the excited-state manifold. Indeed, when 12′-apo-β-carotenal is dissolved in methanol, the spectral features in the region 550–650 nm dominate the spectrum which consists of two major bands, the $A_g^- - nB_u^+$ band with maximum at 515 nm and the ICT band peaking at 587 nm. The intensity ratio of these two bands varies with solvent polarity; the more polar the solvent, the greater the intensity of the ICT band,[21] and this is a general characteristic of transient spectra of carbonyl carotenoids.[5,16,17]

The appearance of the ICT band is accompanied by a significant shortening of the A_g^-/ICT state lifetime as evidenced by a comparison of the kinetics measured within the $A_g^- - nB_u^+$ (*n*-hexane) and ICT (methanol) bands (Fig. 4b). Further insight into the excited-state dynamics is provided by the global fitting results shown in Fig. 5. For both solvents, three decay components are sufficient to obtain good fits. In *n*-hexane, the three components are comparable to those obtained for 12′-apo-β-carotene: the initially excited B_u^+ state decays in 130 fs to populate a hot A_g^- state, which relaxes with a 2.9 ps time constant, and the relaxed A_g^- state then decays to the ground state with a lifetime of 180 ps. In methanol, the component associated with the B_u^+ lifetime is similar at 110 fs,
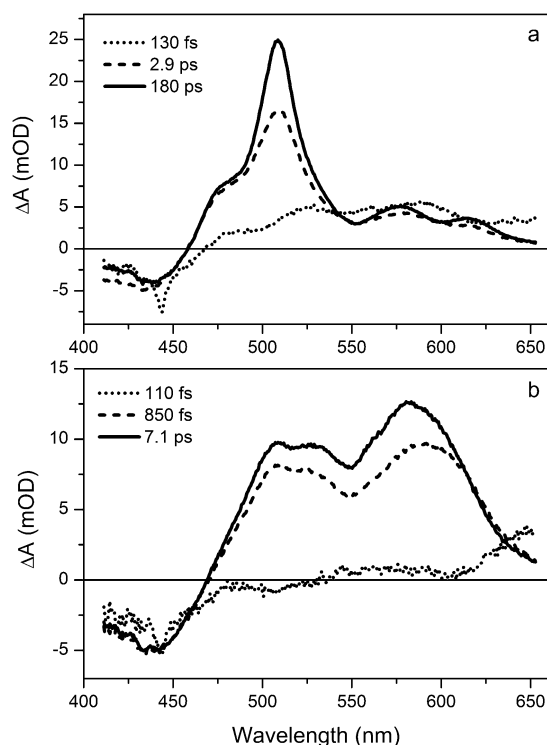
but the subsequent dynamics differ dramatically. Decay of the B_u^+ state generates both $A_g^- - nB_u^+$ and ICT bands. This is usually interpreted in terms of population transfer to a complicated potential surface of a coupled A_g^-/ICT state.[6,10,11] The second, 850 fs component then corresponds to stabilization of the A_g^-/ICT state which subsequently decays to the ground state with a 7.1 ps time constant. The lifetimes extracted from global fitting are in agreement with previous analyses of the solvent-dependent excited-state dynamics of 12′-apo-β-carotenal obtained from both single-wavelength[15,19] and diode-array measurements.[21]

Transient absorption spectra of retinal recorded in *n*-hexane and methanol are shown in Fig. 6 from which it is obvious that despite the structural similarity of retinal and 12′-apo-β-carotenal, the excited-state dynamics of these two molecules are significantly different. Since the initially excited B_u^+ state of retinal has extremely short (56 fs) lifetime in *n*-hexane,[29] the transient features observed 0.2 ps after excitation are mostly associated with the transitions originating from the excited A_g^- state. In contrast to 12′-apo-β-carotenal, this excited A_g^- state spectrum of retinal, which consists of a few bands spanning the whole visible spectral region, decays even in *n*-hexane within the first 2 ps. At later times, however, a new band, associated with T–T transition, appears at 440 nm.[30] This behavior of retinal in *n*-hexane was described earlier,[28–30] and it is explained as follows: the A_g^- state, populated in less than 100 fs from the absorbing B_u^+ state, decays in a few ps to an nπ* state, which has no spectral signature in the visible spectral region, and is a precursor of intersystem crossing to a triplet state. The formation of the triplet state, however, does not occur in methanol. Instead, a broad, featureless band due
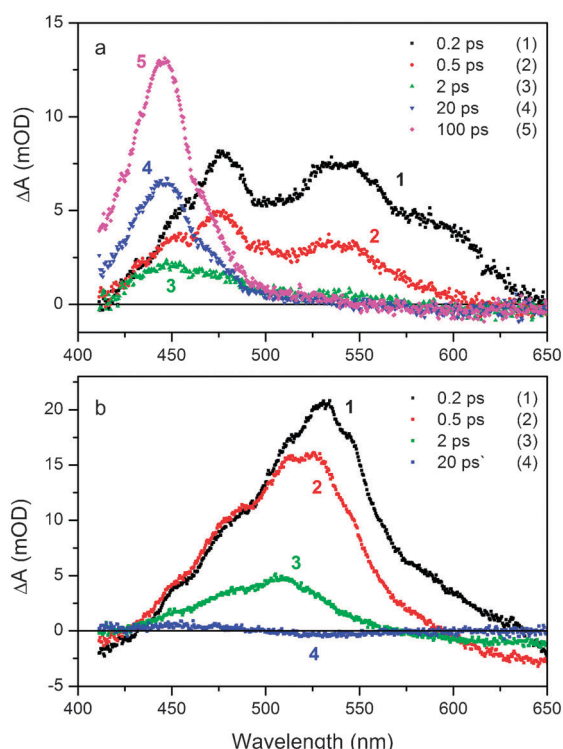
This journal is © the Owner Societies 2011

Phys. Chem. Chem. Phys., 2011, **13**, 10787–10796 | 10791

Fig. 6 Transient absorption spectra of retinal at a few delay times after excitation at 395 nm in *n*-hexane (a) and methanol (b).

to the A_g^- state disappears on a picosecond time scale without any observable long-lived products. It is also worth noting that a clear stimulated emission band, which is absent in *n*-hexane, occurs above 600 nm for retinal in methanol (Fig. 6b).

The fast depopulation of retinal excited states is demonstrated by kinetics shown in Fig. 7. Comparison of the kinetics taken close to the maximum of the transient absorption band associated with the A_g^- state, *i.e.* at 545 nm in *n*-hexane and at 515 nm in methanol, reveals that the decay of the A_g^- state differs in these two solvents. This difference is further demonstrated
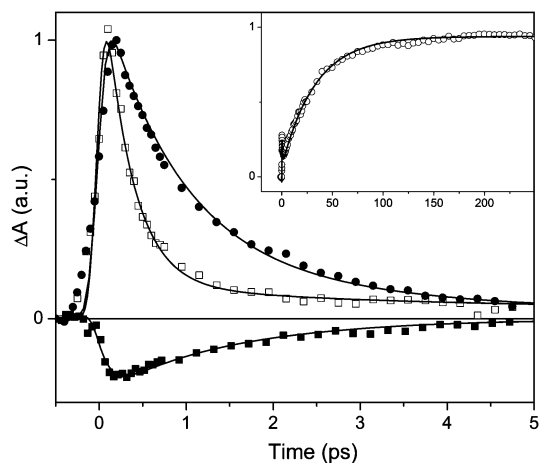

Fig. 7 Kinetics recorded for retinal in *n*-hexane at 545 nm (open symbols), and in methanol at 515 nm (full circles) and 650 nm (full squares). Inset shows the rise of signal at 465 nm in *n*-hexane. Kinetics are normalized to their maxima except the kinetics at 650 nm which is scaled to maintain ratio between signal magnitudes at 515 and 650 nm.
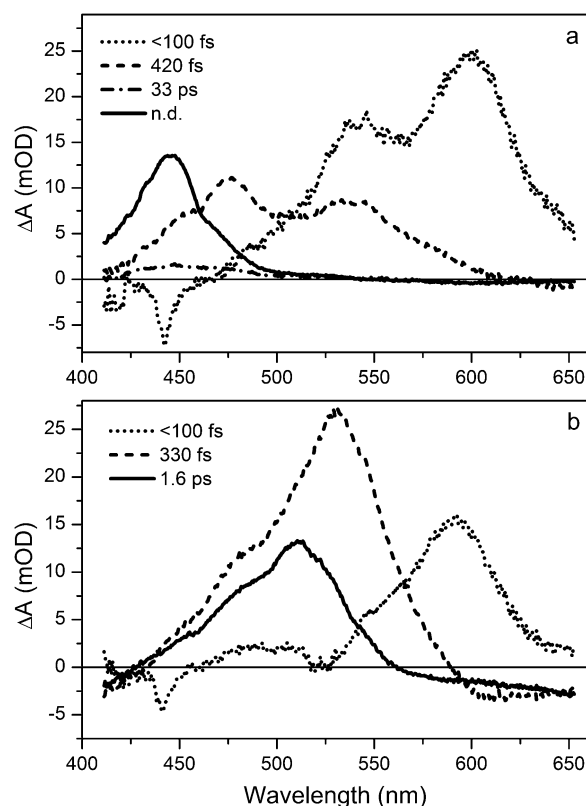

Fig. 8 EADS obtained from global fitting the data measured for retinal in *n*-hexane (a) and methanol (b).

by the global fitting results depicted in Fig. 8. In *n*-hexane, the B_u^+ state initially populated by excitation at 395 nm has a spectral signature peaking around 600 nm. It should be noted that the B_u^+ lifetime of 56 fs for retinal was determined in *n*-hexane,[29] and is beyond the time resolution of our experiments. Consequently, mixing of spectral features associated with the B_u^+ and A_g^- states is the likely reason for the presence of the 550 nm band in both the first and second EADS. In *n*-hexane, the second EADS is associated with the A_g^- state that decays in 420 fs to form the third EADS. It has almost zero amplitude in the 400–650 nm spectral region and is associated with the spectrally silent nπ* state. This EADS then gives way in 33 ps to the final spectrum that is due to the triplet state characterized by the T–T transition peaking at 440 nm.

In methanol, the first EADS due to the B_u^+ state is very similar to that in *n*-hexane, indicating that solvent polarity does not affect the excited state absorption from the B_u^+ state. It decays with less than 100 fs, but the second EADS has a maximum at 545 nm with a weak shoulder at ∼470 nm. The second EADS also contains clear evidence for stimulated emission in the 600–650 nm spectral region. The third EADS, formed in 330 fs, is similar to the second one, except the main peak is slightly blue-shifted to 510 nm. This EADS then decays to zero with a 1.6 ps time constant thus no long-lived species are detected for retinal in methanol.

Discussion

Analysis of absorption spectra shown in Fig. 2 indicates that retinal exhibits features typical for carbonyl carotenoids.

It should be noted that a conjugated carbonyl group has two different effects on absorption spectra. (1) Stabilization of the B_u^+ energy, which is independent of solvent polarity and shifts the absorption maximum toward longer wavelengths.[6] This effect depends solely on the number of conjugated C=O groups and in extreme cases where multiple carbonyls are present may lead to a spectral shift that turns the color of a red-orange carotenoid to blue.[36] (2) Polarity-dependent asymmetric broadening on the long-wavelength side of the absorption spectrum and loss of vibrational structure which are observed exclusively in polar solvents. While the asymmetric broadening is clearly visible in retinal and 12′-apo-β-carotenal, loss of vibrational structure is less pronounced, because the resolution of the vibrational bands decreases with decreasing conjugation length, and this effect is independent of whether the conjugated carbonyl group is present or not.[37] Thus, the absorption spectra clearly show that retinal follows the trend observed for other apo-carotenals.[12,15]

Excited-state dynamics in *n*-hexane

The A_g^- lifetime of apo-carotenals in *n*-hexane becomes longer with decreasing conjugation length, yielding 4.7 ps (4′-apo-β-carotenal),[12] 12 ps (6′-apo-β-carotenal),[25] 21 ps (8′-apo-β-carotenal),[12] and 180 ps (12′-apo-β-carotenal, Fig. 5). The same behavior was observed for a series of carbonyl-containing synthetic peridinin molecules. The A_g^- lifetime in *n*-hexane of these molecules varied from 40 ps to 4.2 ns upon shortening the conjugation from 8LO (L denotes that the carbonyl group is located at a lactone ring) to 5LO.[16] Thus, since the lifetime of the lowest excited state follows the energy gap law,[24] and since the energy gap increases with shortening the conjugation,[38] we may expect the lifetime of the A_g^- state of retinal in *n*-hexane to be significantly longer than that of 12′-apo-β-carotenal. In contrast, the A_g^- lifetime of retinal is only 0.42 ps (Fig. 8) and its final photoproduct is a triplet state, which is not observed for any of the longer apo-carotenals or carbonyl carotenoids.

The deviation of retinal from the trend observed for other apo-carotenals is readily explained by the nπ* state, which due to the short conjugation length of retinal, drops below both the B_u^+ and A_g^- states.[27] The excited state dynamics of retinal in *n*-hexane then result in the three-state model depicted in Fig. 9a: the B_u^+ state decays in <100 fs to the A_g^- state (the value obtained with better time resolution is 56 fs),[29] which is effectively quenched by the nπ* state, resulting in an A_g^- lifetime of 420 fs. The nπ* state then facilitates intersystem crossing to the triplet state.[28–30] For the next longer apo-carotenal in the series, 12′-apo-β-carotenal, the nπ* state lies above B_u^+ state preventing it from quenching the A_g^- state and steering the population to the triplet state. It is interesting to note that 'retinal-like' behavior has never been observed in the peridinin series, though the shortest molecule in that series has conjugation length comparable to retinal.[16,39] This is most likely related to the specific structure of peridinin, which has the conjugated carbonyl group located in a lactone ring and its conjugated C=C chain terminated by an allene group.[40] It is likely that these structural features prevent the nπ* state from affecting the excited-state dynamics even
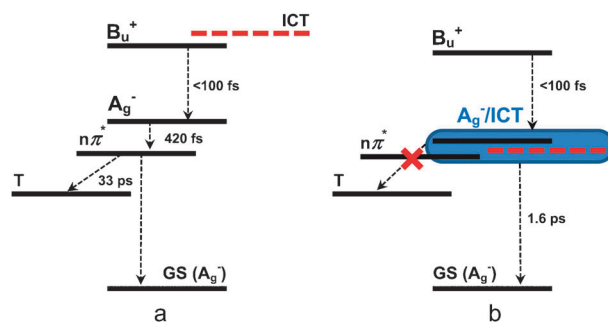

Fig. 9 Relaxation pathways of retinal in *n*-hexane (a) and methanol (b) after excitation of retinal into the B_u^+ state. The dashed line denotes the ICT state whose energy in nonpolar solvent is not known, but it is expected to be significantly higher than in polar solvent. The A_g^-/ICT state in methanol, resulting from coupling of the ICT state to the A_g^- state, is schematically shown as oval including both states. GS, ground state, T, triplet state.

for the shortest known synthetic peridinin analogue. It is also evidenced from the absorption maximum of the shortest peridinin (5LO) which is at ~420 nm in *n*-hexane.[16] Thus, the B_u^+ state lies significantly lower than for retinal.

Origin of the transitions in *n*-hexane

Having established the origin of the short A_g^- lifetime of retinal in *n*-hexane, we may proceed to identify the bands in the transient absorption spectra. We will make use of the reference sample, 12′-apo-β-carotene that lacks the conjugated carbonyl group. Results of global analysis shown in Fig. 3b reveal that the spectrum associated with the A_g^- state consists of a narrow peak at 467 nm that is due to the well-known A_g^-–nB_u^+ transition of carotenoids, and two weak bands at 525 and 580 nm. These bands decay with the same lifetime as the A_g^- state, and thereby represent transitions from the A_g^- state to some state(s) lying below the nB_u^+ state. Since the energy separation between the two weak bands is ~1250 cm^{-1}, thus matching the spacing of vibrational bands in the absorption spectra, these two bands can be assigned to two vibronic transitions associated with the same upper electronic state, which was earlier identified as a state of A_g^+ symmetry.[41]

The transient absorption spectrum of 12′-apo-β-carotenal in *n*-hexane is very similar to that of 12′-apo-β-carotene, except the A_g^-–nB_u^+ transition is shifted to 510 nm, and the vibrational bands of the A_g^-–A_g^+ transition are more pronounced (Fig. 4). Since the A_g^-–A_g^+ transition is forbidden for carotenoids possessing C_{2h} symmetry of their conjugated chain, the intensity of the A_g^-–A_g^+ transition can be considered a measure of asymmetry of the carotenoid molecule. Indeed, for linear non-carbonyl carotenoids with nearly perfect C_{2h} symmetry, only the A_g^-–nB_u^+ transition is seen in the transient absorption spectra. No additional bands are observed at room temperature and only cooling the samples down to 77 K reveals very weak A_g^-–A_g^+ transition.[41] Thus, the conjugated carbonyl group introduces asymmetry into the conjugated system of 12′-apo-β-carotenal, making the A_g^-–A_g^+ transition more intense than seen in 12′-apo-β-carotene.

Considering the transient absorption spectra of 12′-apo-β-carotene and 12′-apo-β-carotenal, we can identify bands in

This journal is © the Owner Societies 2011

Phys. Chem. Chem. Phys., 2011, **13**, 10787–10796 | 10793

the transient absorption spectra of retinal in hexane. Fig. 8 shows that the spectrum of the A_g^- state consists of an $A_g^- - nB_u^+$ transition peaking at 475 nm accompanied by the $A_g^- - A_g^+$ band, which in retinal is significantly stronger than in its longer analogue, 12′-apo-β-carotenal, reflecting even higher degree of asymmetry of retinal. Thus, the degree of asymmetry in apo-carotenals may be understood in terms of the number of conjugated C=C bonds to which the conjugated carbonyl group is attached. The more C=C bonds, the less effect the C=O group has on the overall conjugation. Thus, while for the longest member of the series, 4′-apo-β-carotenal (11 C=C bonds), the influence of the C=O group is negligible, in retinal (5 C=C bonds) the C=O group has a significant effect. This notion of asymmetry may be extended to all carbonyl carotenoids, and it is now established that the degree of asymmetry is directly proportional to magnitude of the polarity-induced effects.[16,39] For carotenoids with two symmetric carbonyl groups, the polarity-induced effects are significantly reduced,[13,17,18] and even four conjugated carbonyls positioned symmetrically with respect to the linear C=C chain cannot produce the polarity-induced effects.[36]

In addition to the assignment of the $A_g^- - nB_u^+$ and $A_g^- - A_g^+$ transitions, the band in the first EADS peaking around 600 nm for retinal in both solvents (Fig. 8) can be assigned to the $B_u^+ - nA_g^-$ transition. This band occurs in the near-IR region for longer carotenoids,[42] and since the energy of all $B_u^+ - A_g^-$ transitions in polyenes and carotenoids increases with decreasing conjugation length,[43] it is shifted to the VIS region for retinal. For 12′-apo-β-carotene and 12′-apo-β-carotenal, the high-energy part of this band is evident in the first EADS at 650 nm (Fig. 3 and 5).

Excited-state dynamics in methanol

For 12′-apo-β-carotene the dynamics in methanol are essentially identical to those in n-hexane, confirming the known fact that non-carbonyl carotenoids are not affected by solvent polarity. However, a significant polarity effect is observed for 12′-apo-β-carotenal. Besides the large change in A_g^- lifetime with solvent observed previously and assigned to a coupling of A_g^- state to an ICT state,[15] the transient absorption spectrum is dominated by a new band centered at 590 nm, which is usually assigned to ICT-like transition[21] and was observed also for other carbonyl carotenoids.[5,6,16,17] Yet, the $A_g^- - nB_u^+$ transition, which dominates the transient absorption spectrum in n-hexane, is still present as evidenced by the second peak at 510 nm (Fig. 4). Because the 510 and 590 nm bands decay with the same time constant (Fig. 5), they are assigned to a coupled A_g^-/ICT state. The A_g^-/ICT coupling is not affected by hydrogen-bonding, because the same lifetimes were observed in aprotic solvent acetonitrile.[19] Thus, the A_g^-/ICT state is generated from the B_u^+ state and further stabilized on $a < 1$ ps time scale (Fig. 5).

Inspection of the transient absorption spectra and global analysis results shown in Fig. 7 and 8 reveals that the same situation occurs for retinal. The $A_g^- - nB_u^+$ band of retinal in methanol at 475 nm is visible only as a weak shoulder on the strong transition that is red-shifted from the $A_g^- - nB_u^+$ band. Although the dynamics are somehow different from those of

12′-apo-β-carotenal, because the main band shifts to blue and loses intensity in 330 fs, the overall similarity justifies assignment of the main band to an ICT-like transition identified previously for other carbonyl carotenoids. This assignment is further justified by the observation of stimulated emission above 600 nm which occurs solely for retinal in methanol. Such stimulated emission is known to occur in a number of carbonyl carotenoids in polar solvents and is now accepted as a reliable marker of the presence of the ICT state.[6,10,11,19] For the carbonyl carotenoids studied so far, this stimulated emission appears in the near-IR region above 800 nm,[6,10,11] but it extends down to 700 nm for 12′-apo-β-carotenal,[21] and it is shifted even farther into the visible spectral region for retinal.

Relaxation pathways of retinal in polar solvent

By comparison of the transient absorption spectra of 12′-apo-β-carotenal and retinal, we can conclude that while excited-state dynamics of retinal in n-hexane can be explained by a three state (B_u^+, A_g^-, $n\pi^*$) model, an ICT state must be included to describe the excited-state dynamics of retinal in methanol. This would readily explain the different A_g^- lifetimes in the different solvents as well as the absence of triplet state formation in methanol. Processes, which occur after excitation of retinal in methanol, are schematically shown in Fig. 9b. The first relaxation step is the same as in n-hexane: the B_u^+ state decays in <100 fs to the A_g^- state. Then, the coupling of the ICT and A_g^- states prevents the population of the $n\pi^*$ state. Instead, the A_g^- state is quenched by the coupling to the ICT state in the same way as it is for longer apo-carotenals or other carbonyl carotenoids. The A_g^-/ICT state is generated as a vibronically hot state, which cools down in 330 fs, and the relaxed A_g^-/ICT state then decays to the ground state in 1.6 ps. The A_g^-–ICT coupling is evidenced by stimulated emission and ICT-like bands that are observed for retinal only when it is dissolved in methanol. It should be noted here that the absence of stimulated emission for retinal in n-hexane after two-photon excitation[44] is consistent with a recent report showing that two-photon excitation of the carbonyl carotenoid fucoxanthin reduces ICT-like features in transient absorption spectra.[45] This further underlines the similarities of excited state dynamics of retinal and carbonyl carotenoids. Bypassing the $n\pi^*$ state also explains the absence of singlet-triplet conversion because the ICT state does not facilitate such a process. It should be noted that the different dynamics observed for retinal in polar and nonpolar solvents cannot be explained solely by the modulation of the energy of $n\pi^*$ states due to hydrogen bonding in protic solvents.[46,47] This is because the dynamics of retinal in the aprotic solvent, acetonitrile, exhibit the same behavior as in the hydrogen-bonding solvent, methanol.[32] Moreover, if the 'standard' A_g^- state were the lowest excited state in a polar solvent, its lifetime should follow the energy gap law and thus be on a time scale of (at least) hundreds of ps.[16]

Coupling of the ICT state to the A_g^- state resolves this contradiction and also explains why the dynamics of retinal are different in polar and nonpolar solvents. It must be noted, however, that the 1.6 ps A_g^-/ICT lifetime of retinal

in methanol is markedly shorter than for other carbonyl carotenoids including apo-carotenals whose shortest A_g^-/ICT lifetimes are in the 7–9 ps range.[5,10,15,16] Since the exact mechanism of the ICT-induced quenching in carotenoids remains unknown, we can only speculate that it is the degree of asymmetry that plays a key role. It is well known that the magnitude of quenching, defined as the difference between the lifetime in the nonpolar and polar solvents, increases with decreasing π-electron conjugation length of the carbonyl carotenoid.[16,17] As described earlier, decreasing the number of the conjugated C=C bonds to which the conjugated C=O bond is attached increases the degree of asymmetry. We have shown that retinal is the most asymmetric carbonyl carotenoid studied so far. Thus, a large magnitude of quenching, resulting in a very short A_g^-/ICT lifetime, should be expected.

Conclusions

In this work we have shown that the excited-state processes in retinal can be consistently explained if an ICT state is included in the relaxation scheme in polar solvents. Comparing the excited-state dynamics of two apo-carotenals, 12′-apo-β-carotenal and 15′-apo-β-carotenal (retinal), in n-hexane and methanol showed common transient spectral features in both molecules. In n-hexane, excitation of the B_u^+ state of both molecules induces ultrafast decay to the A_g^- state, which has a lifetime of 180 ps for 12′-apo-β-carotenal. The A_g^- state is, however, shortened to 420 fs in retinal due to a low-lying nπ* state that efficiently quenches the A_g^- state of retinal and transfers population to a triplet state.

Markedly different behavior is observed in methanol. While the initial B_u^+ to A_g^- relaxation is not affected by solvent polarity, the A_g^- state of 12′-apo-β-carotenal is shortened to 7.1 ps due to coupling to the ICT state, which is indicated by the appearance of characteristic transient absorption bands. The same A_g^-–ICT coupling occurs in retinal, as evidenced by ICT-like transient absorption bands and ICT stimulated emission. The A_g^-/ICT coupling prevents population of the nπ* state, resulting in an absence of retinal triplet population in methanol. Instead, the A_g^-/ICT state decays to the ground state in 1.2 ps. Thus, the results show that a general relaxation scheme employed to explain excited-state dynamics of carbonyl carotenoids can be applied also to retinal. Also, the very short conjugation of retinal supports the notion of asymmetry as a key structural feature controlling the magnitude of the polarity-induced effects.

Acknowledgements

Notes and references

1 T. Polívka and V. Sundström, *Chem. Rev.*, 2004, **104**, 2021–2072.
2 P. Tavan and K. Schulten, *Phys. Rev. B*, 1987, **36**, 4337–4358.
3 K. Schulten and M. Karplus, *Chem. Phys. Lett.*, 1972, **14**, 305–307.
4 T. Polívka and V. Sundström, *Chem. Phys. Lett.*, 2009, **477**, 1–11.
5 H. A. Frank, J. A. Bautista, J. Josue, Z. Pendon, R. G. Hiller, F. P. Sharples, D. Gosztola and M. R. Wasielewski, *J. Phys. Chem. B*, 2000, **104**, 4569–4577.
6 D. Zigmantas, R. G. Hiller, F. P. Sharples, H. A. Frank, V. Sundström and T. Polívka, *Phys. Chem. Chem. Phys.*, 2004, **6**, 3009–3016.
7 J. A. Bautista, R. G. Hiller, F. P. Sharples, D. Gosztola, M. Wasielewski and H. A. Frank, *J. Phys. Chem. A*, 1999, **10**, 2267–2273.
8 S. Stalke, D. A. Wild, T. Lenzer, M. Kopczynski, P. W. Lohse and K. Oum, *Phys. Chem. Chem. Phys.*, 2008, **10**, 2180–2188.
9 D. Kosumi, T. Kusumoto, R. Fujii, M. Sugisaki, Y. Iinuma, N. Oka, Y. Takaesu, T. Taira, M. Iha, H. A. Frank and H. Hashimoto, *Chem. Phys. Lett.*, 2009, **483**, 95–100.
10 D. Zigmantas, T. Polívka, R. G. Hiller, A. Yartsev and V. Sundström, *J. Phys. Chem. A*, 2001, **105**, 10296–10306.
11 D. Zigmantas, R. G. Hiller, A. Yartsev, V. Sundström and T. Polívka, *J. Phys. Chem. B*, 2003, **107**, 5339–5348.
12 F. Ehlers, D. A. Wild, T. Lenzer and K. Oum, *J. Phys. Chem. A*, 2007, **111**, 2257–2265.
13 P. Chábera, M. Fuciman, P. Hříbek and T. Polívka, *Phys. Chem. Chem. Phys.*, 2009, **11**, 8795–8803.
14 J. A. Bautista, R. E. Connors, B. B. Raju, R. G. Hiller, F. P. Sharples, D. Gosztola, M. R. Wasielewski and H. A. Frank, *J. Phys. Chem. B*, 1999, **103**, 8751–8758.
15 D. A. Wild, K. Winkler, S. Stalke, K. Oum and T. Lenzer, *Phys. Chem. Chem. Phys.*, 2006, **8**, 2499–2505.
16 D. M. Niedzwiedzki, N. Chatterjee, M. M. Enriquez, T. Kajikawa, S. Hasegawa, S. Katsumura and H. A. Frank, *J. Phys. Chem. B*, 2009, **113**, 13604–13612.
17 M. M. Enriquez, M. Fuciman, A. M. LaFountain, N. L. Wagner, R. R. Birge and H. A. Frank, *J. Phys. Chem. B*, 2010, **114**, 12416–12426.
18 P. Chábera, M. Fuciman, K. R. Naqvi and T. Polívka, *Chem. Phys.*, 2010, **373**, 56–64.
19 M. Kopczynski, F. Ehlers, T. Lenzer and K. Oum, *J. Phys. Chem. A*, 2007, **111**, 5370–5381.
20 F. Ehlers, T. Lenzer and K. Oum, *J. Phys. Chem. B*, 2008, **112**, 16690–16700.
21 K. Oum, P. W. Lohse, F. Ehlers, M. Scholz, M. Kopczynski and T. Lenzer, *Angew. Chem., Int. Ed.*, 2010, **49**, 2230–2232.
22 R. Englman and J. Jortner, *Mol. Phys.*, 1970, **18**, 145–164.
23 H. A. Frank, A. Cua, V. Chynwat, A. Young, D. Gosztola and M. R. Wasielewski, *Photosynth. Res.*, 1994, **106**, 2083–2092.
24 V. Chynwat and H. A. Frank, *Chem. Phys.*, 1995, **194**, 237–244.
25 Z. F. He, D. Gosztola, Y. Deng, G. Q. Gao, M. R. Wasielewski and L. D. Kispert, *J. Phys. Chem. B*, 2000, **104**, 6668–6673.
26 T. Kouyama and M. Murakami, *Photochem. Photobiol. Sci.*, 2010, **9**, 1458–1465.
27 M. Merchán and R. González-Luque, *J. Chem. Phys.*, 1997, **106**, 1112–1122.
28 S. Takeuchi and T. Tahara, *J. Phys. Chem. A*, 1997, **101**, 3052–3060.
29 K. Ishii, S. Takeuchi and T. Tahara, *Chem. Phys. Lett.*, 2005, **418**, 307–310.
30 S. Yamaguchi and H. Hamaguchi, *J. Phys. Chem. A*, 2000, **104**, 4272–4279.
31 E. J. Larson and C. K. Johnson, *J. Phys. Chem. B*, 1999, **103**, 10917–10923.
32 E. J. Larson, S. J. Pyszczynski and C. K. Johnson, *J. Phys. Chem. A*, 2001, **105**, 8136–8144.
33 R. R. Birge, L. A. Bennett, L. M. Hubbard, H. L. Fang, B. M. Pierce, D. S. Kliger and G. E. Leroi, *J. Am. Chem. Soc.*, 1982, **104**, 2519–2525.
34 I. H. M. van Stokkum, D. S. Larsen and R. van Grondelle, *Biochim. Biophys. Acta, Bioenerg.*, 2004, **1657**, 82–104.
35 H. H. Billsten, J. X. Pan, S. Sinha, T. Pascher, V. Sundström and T. Polívka, *J. Phys. Chem. A*, 2005, **109**, 6852–6859.
36 T. Polívka, H. A. Frank, M. M. Enriquez, D. M. Niedzwiedzki, S. Liaaen-Jensen, J. Hemming, J. R. Helliwell and M. Helliwell, *J. Phys. Chem. B*, 2010, **114**, 8760–8769.
37 R. L. Christensen, M. Goyette, L. Gallagher, J. Duncan, B. DeCoster, J. Lugtenburg, F. J. Jansen and I. van der Hoef, *J. Phys. Chem. A*, 1999, **103**, 2399–2407.

38 R. L. Christensen, E. A. Barney, R. D. Broene, M. G. I. Galinato and H. A. Frank, *Arch. Biochem. Biophys.*, 2004, **430**, 30–36.

39 N. Chatterjee, D. M. Niedzwiedzki, T. Kajikawa, S. Hasegawa, S. Katsumura and H. A. Frank, *Chem. Phys. Lett.*, 2008, **463**, 219–224.

40 N. Chatterjee, D. M. Niedzwiedzki, K. Aoki, T. Kajikawa, S. Katsumura, H. Hashimoto and H. A. Frank, *Arch. Biochem. Biophys.*, 2009, **483**, 146–155.

41 D. Niedzwiedzki, J. F. Koscielecki, H. Cong, J. O. Sullivan, G. N. Gibson, R. R. Birge and H. A. Frank, *J. Phys. Chem. B*, 2007, **111**, 5984–5998.

42 J. P. Zhang, L. H. Skibsted, R. Fujii and Y. Koyama, *Photochem. Photobiol.*, 2001, **73**, 219–222.

43 C. Scriban, B. S. Amagai, E. A. Stemmler, R. L. Christensen and R. R. Schrock, *J. Am. Chem. Soc.*, 2009, **131**, 13441–13452.

44 E. J. Larson, L. A. Friesen and C. K. Johnson, *Chem. Phys. Lett.*, 1997, **265**, 161–168.

45 D. Kosumi, T. Kusumoto, R. Fujii, M. Sugisaki, Y. Iinuma, N. Oka, Y. Takaesu, T. Taira, M. Iha, H. A. Frank and H. Hashimoto, *Chem. Phys. Lett.*, 2009, **483**, 95–100.

46 W. P. Hayes and C. J. Timmons, *Spectrochim. Acta*, 1965, **21**, 529–541.

47 F. C. Grozema and P. T. van Duijnen, *J. Phys. Chem. A*, 1998, **102**, 7984–7989.